# Model for Electricity Generation by Thermoelectric Generators used in Spectrum-Splitting Applications

Ahmed Issa Alnahhal[1,2], Ahmad Halal[1] and Balázs Plesz[1],
[1]Department of Electron Devices
Budapest University of Technology and Economics
Budapest, Hungary

[2]Department of Biomedical Engineering
University of Palestine
Gaza Strip, Palestine

## *Abstract*

*A model of solar thermoelectric generator STEG device is presented which consist of a concentrator part, heat collector part, TEG part and heat sink part. A simulation is carried out for the full spectrum, visible light spectrum (380 nm-750 nm) and near infrared spectrum (750nm-3000nm) of solar radiation in term of concentration. The hot side temperature, cold side temperature and their temperature difference are simulated for each spectrum. Also, the generated voltage, current, output power and the efficiency of the TEG have been evaluated and simulated for each spectrum. The effects of the heat transfer coefficient of the heat sink and concentration levels are included and evaluated. With non-concentrated or at the same concentrated light naturally, the full spectrum resulted in the highest efficiency, but higher concentration levels can compensate the lower power density of filtered light. Also compared to PV cells the efficiency is lower with both the full and the visible spectrum, however in the IR-region it can be competitive to PV-cells, due to its broader absorption spectrum. Due to this TEGs can be a viable alternative for solar cells in applications where the lower wavelength parts of the spectrum are used for different purposes or devices (i.e., high band gap solar cells, plant growth, etc.).*

**Keywords:** Thermoelectric Generator, Solar Spectrum Splitting, Concentrated Spectrum, MATLAB.

## INTRODUCTION

The most used energy resources are limited resources, and they will be depleted quickly due to their widespread use. The use of these resources is likewise detrimental to the ecosystem. The use of solar energy is becoming increasingly vital as the resource issue worsens. Photovoltaics and concentrated solar power are two of the most common technologies for directly harnessing the sun's energy. Furthermore, a significant portion of these resources are squandered as waste heat rather than being transformed into electrical energy. Solar thermoelectric generator STEG is a power generation technology that converts the incoming solar radiation into thermal energy, and transforms this thermal energy directly into electricity [1]. Thermoelectric generator (TEG) units consist of n- and p-type semiconductor materials which are connected electrically in series and thermally in parallel [2]. A highly efficient TEG device will depend on the electrical and thermal characteristics of the used semiconductor materials as thermal conductivity, electrical conductivity and Seebeck coefficient which define the figure of merit (ZT) of the TEG device as

$$ZT= \frac{s^2\sigma}{K} T \quad (1)$$

Where s, σ, k and T are the Seebeck coefficient, electrical conductivity, thermal conductivity, and average temperature, respectively [3]. The conversion efficiency of TEGs is limited by two major factors; the Carnot cycle efficiency, which establishes a theoretical upper constraint on the efficiency of thermal energy conversion to work and the efficiency of the thermoelectric effect. Carnot efficiency is $\Delta T/T_h$, where $T_h$ is the temperature of the hot side and $\Delta T$ is the temperature difference between the hot and cold sides [4]. As a result, the overall efficiency of a thermoelectric device is governed as follows

$$\eta= \frac{\Delta T}{T_H} \frac{(1+ZT)^{\frac{1}{2}}-1}{(1+ZT)^{\frac{1}{2}}-\frac{T_C}{T_H}} \quad (2)$$

Where $T_C$ is the cold-side temperature, $T_H$ is the hot-side temperature, $\Delta T$ the temperature difference $T_H$ - $T_C$ and

ZT is the thermoelectric material's figure of merit [5-6]. The lower the thermal conductivity and higher the electrical conductivity and Seebeck coefficient of the material, the higher ZT and the more efficient the TEG device. Higher temperature differences across the TEG terminals also increase the TEG's efficiency. Therefore, concentrated solar thermoelectric generator (CSTEG) is introduced in which the sun's energy is concentrated. The area of the thermoelectric module is substantially less than in flat-plate systems because the focusing optics focus the light. The reduced size of used semiconductor materials results in lower cost, in which the expensive semiconductor materials are replaced by cheap ones, such as glass mirrors or lenses, steel, aluminum, and plastics. Bismuth Telluride ($Bi_2Te_3$) is a common thermoelectric generator material which can be used up to temperatures of 350°C [7]. Their efficiency is less than 10%. Many thermoelectric materials are currently being investigated to increase and optimize power generation, also recent advancements in ZT offers significant potential in the development of new generation as well [8]. Ideas for solar thermoelectric generators and photovoltaic thermoelectric hybrid systems have been developed in recent years as thermoelectric technology has progressed [9,10]. Thermoelectric devices have several advantages over conventional power-generation methods [11]: TEGs are silent solid-state devices with no moving parts, ecologically friendly, scalable from tiny to large heat sources, and very reliable. They also have a longer lifespan and the ability to create electrical energy from low-grade thermal energy. This paper contains four sections. The second section is methodology, the third section is the results and discussion, and the fourth section is the conclusion.

## METHODOLOGY

Fig. 1 shows a schematic diagram of a CSTEG system in which a concentration lens concentrates the solar radiation into the heat collector. The heat collector collects the solar energy and transfer it to the hot side of TEG module. A heat sink is used to remove the heat from the other terminal of the TEG module for temperature gradient establishing.

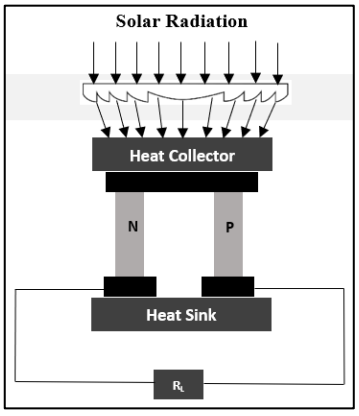

Fig. 1: Concentrated Solar Thermoelectric Generator CSTEG

### Thermoelectric Generator Model

The heat collected by the TE module's hot junction can be represented as [12]

$$Q_H = \alpha_{HC} E_{TEG} - Q_{rad} - Q_{conv} \quad (3)$$

Where $\alpha_{HC}$ is the heat collector absorptivity, $E_{TEG}$ is the input solar energy of heat collector, $Q_{rad}$ and $Q_{conv}$ are the heat collector's radiation and convection heat losses respectively. The heat collected by the hot junction which is equal to the heat transferred by heat collector, and the heat removed by the thermoelectric cold junction [12] are as follow:

$$Q_H = K_{HC}(T_{HC} - T_H) \quad (4)$$
$$Q_C = h_c A_{HS}(T_C - T_{Coolant}) \quad (5)$$

Where $K_{HC}$ represents the heat collector conductivity, $h_C$ is the heat transfer coefficient, $A_{HS}$ is area of heat sink, $T_{HC}$, $T_H$, $T_C$ and $T_{Coolant}$ are heat collector, hot side, cold side and coolant temperatures. The classic formulae for absorbed and removed heat [13] based on the Seebeck, Thomson, and Peltier effects are as follows:

$$Q_H = (K_p + K_n)(T_H - T_C) - \frac{1}{2} I^2 (R_p + R_n) + (S_p - S_n) I T_H \quad (6)$$
$$Q_C = (K_p + K_n)(T_H - T_C) + \frac{1}{2} I^2 (R_p + R_n) + (S_p - S_n) I T_C \quad (7)$$

Where I is the current supplied by the Seebeck effect voltage, $S_{n,p}$, $R_{n,p}$ and $K_{p,n}$ are the Seebeck coefficient, electrical resistance and thermal conductance of TEG n- and p-type legs respectively [14] in which

$$R_{n,p} = \frac{L}{A_{n,p}\sigma_{n,p}} \quad (8)$$
$$K_{n,p} = \frac{A_{n,p}k_{n,p}}{L} \quad (9)$$

Where $A_{n,p}$ is the n-type and p-type legs cross-section area, $\sigma_{n,p}$ and $k_{n,p}$ are n- and p-type legs electrical and thermal conductivity respectively. The current I supplied by the Seebeck voltage and the TEG output power [15] are as follow:

$$I = \frac{V_{TEG}}{R_L + R_{TEG}} \quad (10)$$
$$P_{TEG} = I^2 R_{TEG} \quad (11)$$

By setting $R_L = R_{TEG}$, the maximum efficiency of the TEG subsystem is as [15]

$$\eta_{TEG} = \frac{P_{TEG}}{E_{TEG}} \quad (12)$$

### Spectrum-Based Electricity Generation

A CSTEG model is presented using the forementioned equations in MATLAB. The output power of the CSTEG system is determined by the spectrum and intensity of the incident sunlight, as well as the electrical and thermal characteristics of the TEG thermocouple. The solar radiation spectrum has been divided into three parts, full spectrum, visible spectrum (400 nm-780 nm) and near infrared spectrum (780 nm-3000 nm). The output power

and efficiency of the CSTEG has been evaluated and simulated for each spectrum in terms of concentration levels. The solar spectrum-based energy is calculated in (13) where $\eta_{opt}$ is the concentrator efficiency, F(λ) the irradiance spectrum, $\lambda_1$ and $\lambda_2$ are the spectrum wavelengths limits.

$$E_{TEG} = \int_{\lambda_1}^{\lambda_2} \eta_{opt} A_{HC} C_g F(\lambda)\, d\lambda \quad (13)$$

The simulation has been performed for natural convection heat transfer coefficient of 2.5 W/(m$^2$K) [16] and using the parameters in table I and under the following assumptions; the TEG module's contact resistances are neglected and the Seebeck coefficient, electrical and thermal conductivity of the TEG legs materials are the same at the hot and cold sides.

| Sy. | Description | Value |
|---|---|---|
| | **Optical** | |
| $\eta_{opt}$ | Optical Efficiency | 0.9 |
| $C_g$ | Concentration ratio | 50-150 suns |
| | **Heat Collector [12]** | |
| $A_{HC}$ | Surface Area | 50 um$^2$ |
| $K_{HC}$ | Thermal Conductivity | 0.2 W/K |
| $\alpha_{HC}$ | Absorptivity | 0.95 |
| $\varepsilon_{HC}$ | Emissivity | 0.08 |
| | **TEG [17]** | |
| $L_{p,n}$ | Length of p and n-Type Leg | 5mm |
| $W_{pn}$ | Width of p and n-Type Leg | 5mm |
| $H_{p,n}$ | Height of p and n-Type Leg | 5mm |
| $\sigma_p$ | p - Leg Electrical Conductivity | 76103 $(\Omega m)^{-1}$ |
| $\sigma_n$ | n - Leg Electrical Conductivity | 89365 $(\Omega m)^{-1}$ |
| $k_p$ | p - Leg Thermal Conductivity | 1.265W/(mK) |
| $k_n$ | n - Leg Thermal Conductivity | 1.011W/(mK) |
| $s_p$ | Seebeck Coefficient of p-Leg | $2.037\times10^{-4}$ V/K |
| $s_n$ | Seebeck Coefficient of n-Leg | $-1.721\times10^{-4}$ V/K |
| | **Heat Sink** | |
| $A_{HS}$ | Surface Area | 50 um$^2$ |
| $h_c$ | Heat transfer Coefficient | 1000 W/m$^2$K |

Table I. Data Parameters Used in the CSTEG Model

## RESULTS AND DISCUSSION

Fig. 2 shows the temperature, heat collector heat flux and efficiency of CSTEG of full, visible light and near infrared spectrums at concentration ratio of 100 suns. Fig. 2 (a) shows hot, cold side temperatures and temperature difference. The hot side temperature of full spectrum is higher than the visible light and near infrared spectrums. Also, the cold side temperature of full spectrum is higher than the others. The difference of hot and cold side temperatures of full, visible light and near infrared spectrums are 218.57 K, 123.96 K and 103.47 K respectively. Fig. 2 (b) depicts that the heat flux of heat collector of full, visible light and near infrared spectrums are 4.1968 W, 2.1887 W and 1.7929 W respectively. While fig. 2 (c) indicates that the efficiency of the CSTEG is the highest with the full spectrum, while the near infrared spectrum has the lowest efficiency, and the visible light has an efficiency in between. Fig. 3 shows the temperature and efficiency of CSTEG of visible light and near infrared spectrums at concentration levels of 50, 75, 100, 125 and 150 suns and a heat transfer coefficient of the heat sink of 1000 W/m$^2$K.

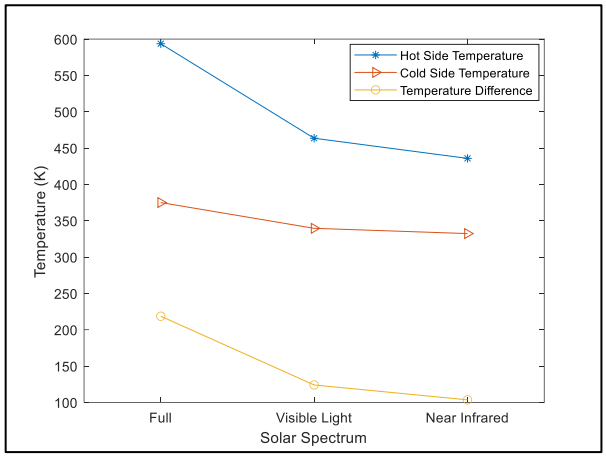


(a)

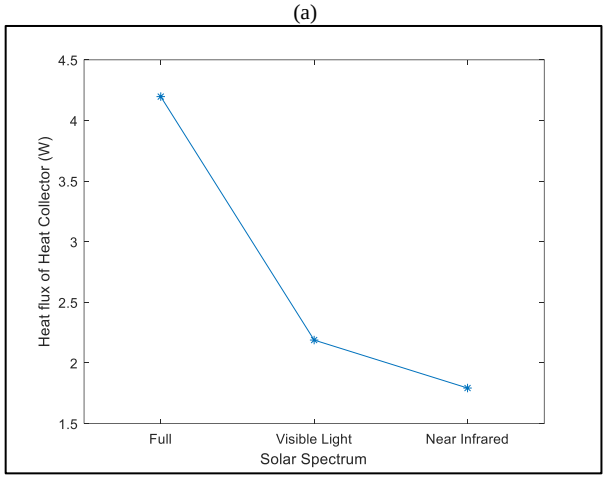


(b)

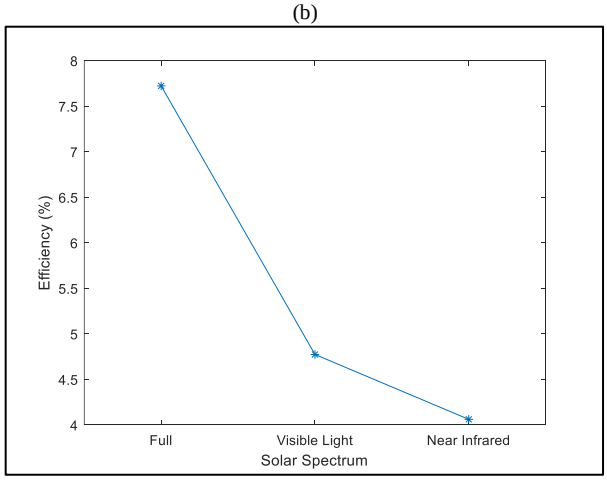


(c)

Fig. 2: Thermoelectric Generator a) Temperature -Solar Spectrums, b) Heat Flux – Solar Spectrums and c) Efficiency-Solar Spectrums at heat transfer coefficient of 1000 W/m$^2$K.

Fig. 3 (a) shows the hot side temperature, cold side temperature and temperature difference of concentrated visible light spectrum. The hot side temperature increases almost linearly with the concertation levels. The cold side temperature shows the same tendency but with a lower slope, thus the temperature difference is increasing. Fig. 3

(b) depicts the hot side temperature, cold side temperature and temperature difference of concentrated near infrared spectrum. The visible light spectrum heats the TEG more than the near infrared spectrum. Therefore, Fig. 3 (c) indicates that the efficiency of CSTEG at visible light spectrum is higher than its efficiency at near infrared spectrum.

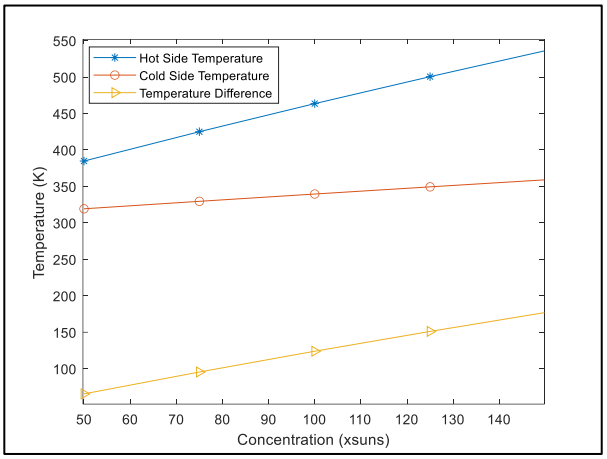


(a)

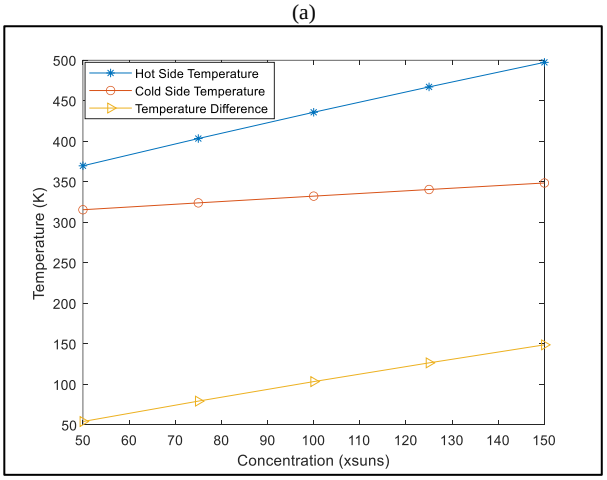


(b)

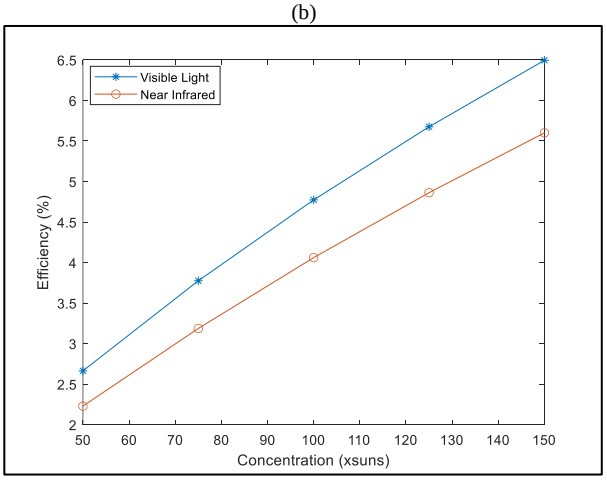


(c)

Fig. 3: Thermoelectric Generator a) Temperature - Concentration of visible light spectrum, b) Temperature – Concentration of near infrared spectrum and c) Efficiency-Concentration at heat transfer coefficient of 1000 W/m$^2$K for the heat sink.

Comparing Fig. 3 (C) with Fig. 2 (C), the efficiency of TEG at visible light and infrared spectrums at concentration of 100 suns are 4.77% and 4.06% respectively, while its efficiencies at concentration of 150 suns are 6.49% and 5.60% respectively. While the efficiency of TEG at full spectrum with concentration 100 suns is 7.72%. It can be seen that the efficiency of the TEG at visible light and near infrared spectrums at concentration level of 150 suns approach the efficiency of TEG at full spectrum with concentration 100 suns. Thus, a higher concentration levels can compensate the lower power density of filtered light. The hot side, cold side temperatures and efficiency values of the three spectrums with concentrations are tabulated in Table II. Fig. 4 reveals the temperature and efficiency of CSTEG of full, visible light and near infrared spectrums at concentration level of 100 suns and a heat transfer coefficient of the heat sink of 1000 W/m$^2$K, 5000 W/m$^2$K and 10000 W/m$^2$K.

| | 50 | 75 | 100 | 125 | 150 |
|---|---|---|---|---|---|
| Visible Light Spectrum | | | | | |
| $T_H$ (K) | 384.7 | 424.9 | 463.5 | 500.5 | 536.1 |
| $T_C$ (K) | 319.2 | 329.5 | 339.5 | 349.3 | 359.0 |
| $\Delta T$(K) | 65.4 | 95.4 | 123.9 | 151.1 | 177.1 |
| $\boldsymbol{\eta}$ (%) | 2.66 | 3.77 | 4.77 | 5.67 | 6.49 |
| Near Infrared Spectrum | | | | | |
| $T_H$ (K) | 369.7 | 403.3 | 435.7 | 467.0 | 497.3 |
| $T_C$ (K) | 315.5 | 323.9 | 332.3 | 340.4 | 348.5 |
| $\Delta T$(K) | 54.2 | 79.3 | 103.4 | 126.5 | 148.8 |
| $\boldsymbol{\eta}$ (%) | 2.22 | 3.18 | 4.06 | 4.86 | 5.60 |

Table II. Hot Side and Cold Side Temperatures and the TEG Efficiency of Filtered Spectrums with Different Concentration Levels.

Fig. 4 (a) and (b) show that the hot side and cold side temperature of full, visible light and near infrared spectrums are decreased as the heat transfer coefficient increases. The decrease in cold side temperature is more significant than the decrease in hot side temperature, thus their difference increases. It also shows that the decrease of hot side temperature and cold side temperature is more significant as the heat sink's heat transfer coefficient is increased from 1000 W/m$^2$K to 5000 W/m$^2$K than if it increased from 5000 W/m$^2$K to 10000 W/m$^2$K.

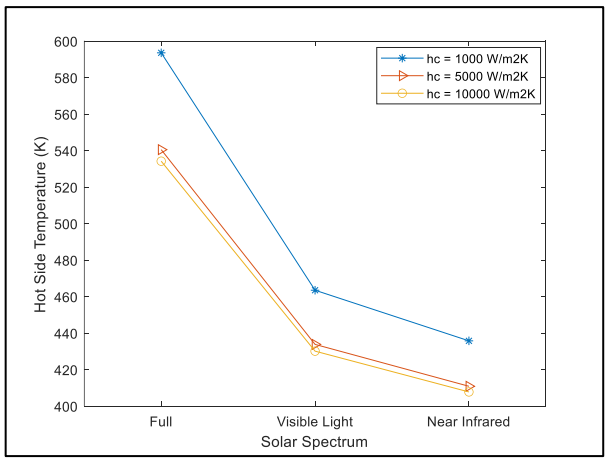


(a)

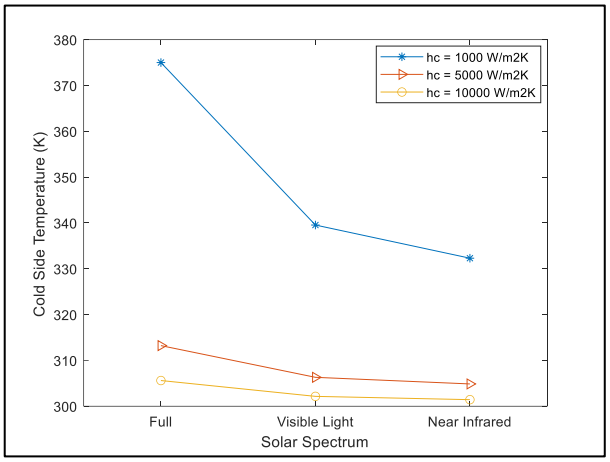


(b)

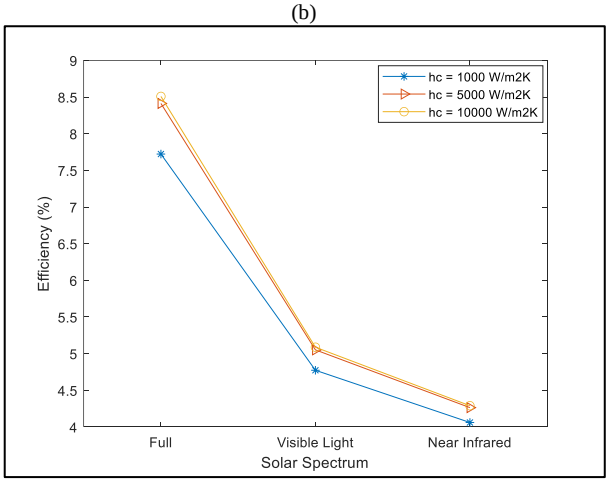


(c)

Fig. 4: Thermoelectric Generator a) Hot side Temperature - Solar Spectrums, b) Cold Side temperature – Solar Spectrums and c) Efficiency- Solar Spectrums at different heat transfer coefficient values.

That is why Fig. 4 (c) indicates that the increase of CSTEG efficiency at each spectrum is more significant as the heat transfer coefficient increased from 1000 W/m$^2$K to 5000 W/m$^2$K. Table III tabulates the hot side and cold side temperatures, their difference and efficiency values of TEG for the three solar spectrums at concentration level of 100 suns and heat sink's heat transfer coefficient of 1000 (W/m$^2$K), 5000 (W/m$^2$K) and 10000 (W/m$^2$K).

| | $h_c$ (W/m$^2$K) | $T_H$ (K) | $T_C$ (K) | $\eta$ (%) |
|---|---|---|---|---|
| Full Spectrum | 1000 | 593.57 | 375.00 | 7.7224 |
| | 5000 | 542.08 | 313.33 | 8.5205 |
| | 10000 | 535.72 | 305.66 | 8.6184 |
| Visible light | 1000 | 463.50 | 339.54 | 4.7731 |
| | 5000 | 433.83 | 306.30 | 5.0513 |
| | 10000 | 430.13 | 302.15 | 5.0875 |
| Near Infrared | 1000 | 435.77 | 332.30 | 4.0608 |
| | 5000 | 410.88 | 304.86 | 4.2636 |
| | 10000 | 407.78 | 301.43 | 4.2898 |

Table III. Hot Side and Cold Side Temperatures and the TEG Efficiency of full and Filtered Spectrums at Different Heat Sink's Heat Transfer Coefficient Values.

## CONCLUSION

A model of the TEG device is presented which consist of a concentration part, heat collector part, TEG part and heat sink part. A simulation is carried out for the full spectrum, visible light spectrum (380 nm-750 nm) and near infrared spectrum (750nm-3000nm) of solar radiation. The hot side temperature, cold side temperature and temperature difference between them are simulated at each spectrum. Also, the generated output power and the efficiency of the TEG have been evaluated and simulated at each spectrum. The effects of the heat transfer coefficient of the heat sink and concentration ratio are included and evaluated. Increasing the heat transfer of the heat sink decreased the temperature of cold side of the TEG. Thus, it was shown that the heat extraction capacity of the heat sink is one of the most important limitations of TEG system performance. The results showed that higher concentration levels can compensate the lower power density of filtered light. Also compared to PV cells, the efficiency is lower with both the full and the visible spectrum, however in the IR-region it can be competitive to PV-cells, due to its broader absorption spectrum. Due to this TEGs can be a viable alternative for solar cells in applications where the lower wavelength parts of the spectrum are used for different purposes or devices (i.e., high band gap solar cells, plant growth etc.) by splitting the spectrum between them.

## ACKNOWLEDGEMENTS

The research reported in this paper and carried out at Budapest University of Technology and Economics was partially supported by the Stipendium Hungaricum Scholarship Program of the Hungarian Government and the project number 2020-1.1.2-PIACI-KFI-2021-00242 of the National Research, Development, and Innovation Office (NKFIH).

## REFERENCES

[1] Lee, Ho Sung: *Thermal design: heat sinks, thermoelectrics, heat pipes, compact heat exchangers, and solar cells*, John Wiley & Sons, 2010.

[2] Rowe, David Michael: *CRC handbook of thermoelectrics*, CRC press, 2018.

[3] Rowe, David Michael: *Thermoelectrics handbook: macro to nano*, CRC press, 2018.

[4] Dousti, Mohammad Javad, Antonio Petraglia, and Massoud Pedram: Accurate electrothermal modeling of Thermoelectric Generators, Proc. DATE15 (Grenoble, 2015), 1603-1606.

[5] Kim, Hee Seok, Weishu Liu, Gang Chen, Ching-Wu Chu, and Zhifeng Ren: Relationship between thermoelectric figure of merit and energy conversion efficiency, Proceedings of the National Academy of Sciences 112, 2015, 8205-8210.

[6] Snyder, G. Jeffrey: Application of the compatibility factor to the design of segmented and cascaded thermoelectric generators, Applied physics letters 84, 2004, 2436-2438.

[7] Mamur, Hayati, M. R. A. Bhuiyan, Fatih Korkmaz, and Mustafa Nil.: A review on bismuth telluride (Bi2Te3) nanostructure for thermoelectric applications, Renewable and Sustainable Energy Reviews 82, 2018, 4159-4169.

[8] Zoui, Mohamed Amine, Saïd Bentouba, John G. Stocholm, and Mahmoud Bourouis.: A review on thermoelectric generators: Progress and applications, Energies 13, 2020, 3606.

[9] Scherrer, H., L. Vikhor, B. Lenoir, A. Dauscher, and P. Poinas: Solar thermolectric generator based on skutterudites, Journal of Power Sources 115, 2003, 141-148.

[10] Kraemer, Daniel, L. Hu, A. Muto, X. Chen, G. Chen, and M. Chiesa: Photovoltaic-thermoelectric hybrid systems: A general optimization methodology, Applied Physics Letters 92, 2008, 243503.

[11] Mamur, Hayati, and Rasit AHISKA.: A review: Thermoelectric generators in renewable energy, International Journal of Renewable Energy Research (IJRER) 4, 2014, 128-136.

[12] Ju, Xing, Zhifeng Wang, Gilles Flamant, Peng Li, and Wenyu Zhao: Numerical analysis and optimization of a spectrum splitting concentration photovoltaic–thermoelectric hybrid systém, Solar energy 86, 2012, 1941-1954.

[13] Babu, Challa, and P. Ponnambalam: The theoretical performance evaluation of hybrid PV-TEG systém, Energy conversion and management 173, 2018, 450-460.

[14] Dhoopagunta, Shripad: *Analytical modeling and numerical simulation of a thermoelectric generator including contact resistances*, 2016.

[15] Li, Peng, Lanlan Cai, Pengcheng Zhai, Xinfeng Tang, Qingjie Zhang, and M. Niino: Design of a concentration solar thermoelectric generator, Journal of electronic materials 39, 2010, 1522-1530.

[16] Kosky, Philip, Robert T. Balmer, William D. Keat, and George Wise.: *Exploring engineering: an introduction to engineering and design*, Academic Press, 2015.

[17] Li, Zhi, Wenhao Li, and Zhen Chen: Performance analysis of thermoelectric based automotive waste heat recovery system with nanofluid coolant, Energies 10, 2017, 1489.

Addresses of the authors

Ahmed Issa Alnahhal, 1117 Budapest, Magyar tudósok krt. 2, Budapest, Hungary, aalnahhal@edu.bme.hu
Ahmad Halal, 1117 Budapest, Magyar tudósok krt. 2, Budapest, Hungary, ahmadhalalftesah@edu.bme.hu
Balazs Plesz, 1117 Budapest, Magyar tudósok krt. 2, Budapest, Hungary, plesz.balazs@vik.bme.hu